HAL open science

Evidence of niche partitioning among bacteria living on plastics, organic particles and surrounding seawaters

C. Dussud, A.L. Meistertzheim, P. Conan, M. Pujo-Pay, M. George, P. Fabre, J. Coudane, P. Higgs, A. Elineau, M.L. Pedrotti, et al.

To cite this version:

C. Dussud, A.L. Meistertzheim, P. Conan, M. Pujo-Pay, M. George, et al.. Evidence of niche partitioning among bacteria living on plastics, organic particles and surrounding seawaters. Environmental Pollution, 2018, 236, pp.807-816. 10.1016/j.envpol.2017.12.027 . hal-04186967

HAL Id: hal-04186967

https://hal.science/hal-04186967v1

Submitted on 25 Aug 2023

HAL is a multi-disciplinary open access archive for the deposit and dissemination of scientific research documents, whether they are published or not. The documents may come from teaching and research institutions in France or abroad, or from public or private research centers.

L'archive ouverte pluridisciplinaire **HAL**, est destinée au dépôt et à la diffusion de documents scientifiques de niveau recherche, publiés ou non, émanant des établissements d'enseignement et de recherche français ou étrangers, des laboratoires publics ou privés.

Distributed under a Creative Commons Attribution 4.0 International License

Evidence of niche partitioning among bacteria living on plastics, organic particles and surrounding seawaters

Dussud C[1], Meistertzheim AL[1], Conan P[1], Pujo-Pay M[1], George M[2], Fabre P[2], Coudane J[3], Higgs P[4], Elineau A[5], Pedrotti ML[5], Gorsky G[5], Ghiglione JF[1]*

[1]Sorbonne Universités, CNRS, UPMC Univ Paris 06, UMR 7621, Laboratoire d'Océanographie Microbienne, Observatoire Océanologique de Banyuls, Banyuls sur mer, France

[2]Laboratoire Charles Coulomb (L2C), Univ. Montpellier, CNRS, Montpellier, France.

[3]Institut des Biomolécules Max Mousseron, CNRS UMR5247, Université de Montpellier, Ecole Nationale Supérieure de Chimie de Montpellier, BP 14491, F-34093 Montpellier cedex5

[4]Symphony Environmental Ltd, Borehamwood, Hertfordshire WD6 1JD, UK.

[5]Sorbonne Universités, CNRS, UPMC Univ Paris 06, UMR 7093, Laboratoire d'Océanographie de Villefranche, Villefranche sur mer, France

***Corresponding author:**

JF Ghiglione, Laboratoire d'Océanographie Microbienne, Observatoire Océanologique de Banyuls, Avenue Fontaulé, F-66650 Banyuls/mer, France. Tel.: + 33 (0) 4 68 88 73 16. E-mail address: ghiglione@obs-banyuls.fr

Note : légendes des figures à la fin de la publication.

Abstract

The Mediterranean Sea is one of the most plastic-polluted zone and offer a unique opportunity to test the hypothesis of bacterioplankton partitioning between free-living (FL), organic particle-attached (PA) and the recently introduced plastic marine debris (PMD). The large set of samples taken during the *Tara*-Mediterranean expedition revealed for the first time a clear niche partitioning between the three co-occurring communities and marked originality in the PMD fraction. Bacterial counts in PMD presented higher cell enrichment factors than generally observed for PA fraction, when compared to FL bacteria in the surrounding waters. Taxonomic diversity was also higher in the PMD communities, where higher evenness indicated a favorable environment for a very large number of species. *Cyanobacteria* were particularly overrepresented in PMD, together with essential functions for biofilm formation and maturation. The consistent distinction of community structure between the three lifestyles, that exceeded the large-scale geographical variation in the Western Mediterranean basin, support a new trade-off for the maintenance of a large diversity of bacterioplankton in the Oceans. 'Plastic specific bacteria' recovered only on the PMD represented half of the OTUs, thus forming a distinct biota that should be further considered for understanding microbial biodiversity in changing marine ecosystems.

Keywords: microbial ecotoxicology, plastisphere, biofouling

***Capsule**:* This study is the first description of bacterial abundance and diversity on plastic marine debris (PMD) in the Mediterranean Sea; it describes PMD as a particular biota for marine bacteria compared to particle-attached and free-living fractions in surrounding waters.

Introduction

Plastic litter have become the most common form of marine debris and a growing global pollution concern, affecting marine ecosystems and economic activities (Gregory, 2009). The discovery of five large-scale accumulation areas of floating PMD in the subtropical ocean gyres has captured worldwide attention, which often refers to these zones as "great garbage patches" (Cózar *et al.*, 2014; Eriksen *et al.*, 2014). These accumulation areas are dominated by plastic pieces, mainly smaller than 5 mm, commonly referred to as "microplastics" (Andrady, 2011; Law and Thompson, 2014). Recent studies have demonstrated that the Mediterranean Sea can be regarded as another great accumulation region with average concentration of more than 200 000 items km^{-2}, comparable to subtropical oceans gyres (Lebreton *et al.*, 2012; Pedrotti *et al.*, 2016). The accumulation of floating plastic in the Mediterranean Sea is explained by the high human density pressure together with the hydrodynamics of this semi-enclosed basin with residence time of 70 years (Durrieu de Madron *et al.*, 2011).

Bacterioplankton represent the most abundant organisms in seawater where they are also the main actors of nutrient regeneration and carbon cycling by converting organic matter to biomass, which supplies microbial food webs and transfers carbon and energy to higher trophic levels (Gasol *et al.*, 2008). Dissolution and degradation of 75% of the organic particles sinking to the sea floor revealed the key role played by PA bacteria in the regulation of the carbon storage by the Oceans (Farooq and Malfatti, 2007; Mével *et al.*, 2008). Particulate organic carbon and more precisely "phycospheres" and "detritospheres" represent micro-patches of concentrated substrates that are hot spots for pelagic bacterial processes (Ghiglione *et al.*, 2009). PA bacteria differ from the surrounding FL fraction in many aspects, including cell abundance, morphology, diversity and metabolic activities (Pulido-Villena *et al.*, 2014; Simon *et al.*, 2002). Microplastics may be considered as new particles recently

introduced within the last 60 years in the Oceans, which offer novel habitats for bacteria and enhance their dispersal over long ways by drifting with currents and winds (Lebreton *et al.*, 2012). Recently, Zettler *et al.* (2013) introduced the term "plastisphere" to describe the very diverse PMD-associated microorganisms, which were found in the seawater sub-surface to differ from the surrounding FL bacteria. Seafloor plastisphere was also found to be genetically unique from the FL water-column bacteria and in addition, they were distinct from the sediment communities in the North Sea (De Tender *et al.*, 2015).

The purpose of this study was first to test the hypothesis of the existence of specific communities associated to PMD particles compared to the PA bacteria. This question is not trivial since any surfaces exposed to seawater are rapidly colonized by bacteria and generally form biofilms (Siboni *et al.*, 2007; Lobelle and Cunliffe, 2011). Because the few studies so far on floating microplastics collected at Sea only compared the PMD to FL bacteria (Zettler *et al.*, 2013, 2015), the question of the existence of a 'plastic-specific' community in contrast to the PA fraction is still open. Here, we provide microscopic counts together with a large dataset of 16S metabarcoding of bacteria living in the PMD, PA and FL fractions collected during the *Tara*-Mediterranean expedition. We also used a computational approach to predict the potential functional differences between the three communities. Finally, we investigated the influence of the location-dependent environmental factors together with the plastic-related properties as potential drivers of the plastisphere characteristics.

Materials and methods

Plastic and surrounding seawater sampling

Samples were taken during the *Tara*-Mediterranean expedition (April-November 2014) aboard the RV *Tara*. PMD were recovered from 32 manta trawls (mesh size 333 µm) carried out in the Western Mediterranean Sea (Figure 1). A subset of these fragments was sorted with sterilized forceps, rinsed with sterile seawater and immediately frozen for further physical, chemical and bacterial diversity analysis. For microscopic observations, PMD were fixed for at least 20 min at room temperature with 2% (v/v) glutaraldehyde (final concentration) before freezing. A conductivity-temperature-fluorescence-depth profiler (CTD – SeaBird SBE 19) was deployed at each of the 32 stations, together with Niskin bottle for surface seawater collection. A fractionation procedure was performed onboard in one step for 2 L seawater sequential filtration through 3 µm-pore size (PA fraction) and 0.2 µm-pore size (FL fraction) polycarbonate filters (47mm diameter, Nucleopore) using a peristaltic pump (pressure <100 mbar) and filters were subsequently frozen until further DNA extraction, as previously described (Ghiglione et al. 1999).

Physical and chemical characterization of the PMD

The one-dimensional area of the surface, the major length and circularity of the individual PMD were determined using ZooScan system (Hydroptic Ltd., EMBRC France) (Gorsky *et al.*, 2010). Fourier Transform Infrared Spectroscopy (FTIR) analysis was performed on the individual PMD using Spectrum 100 equipped with an ATR attenuated total reflectance (Perkin-Elmer) and compared to references for identification of the nature of the polymer. Carbonyl index values were determined as the ratio of the peak intensity at 1,715 cm^{-1} to the peak intensity at 1,460 cm^{-1}, as previously described (Selke *et al.*, 2015).

Microscopic observations

Bacteria were enumerated on 70 plastic pieces sampled at 22 stations (from 1 to 4 pieces per manta, when microscopic observation was possible) by epifluorescence microscopy using an Olympus AX-70 PROVIS after 4', 6-diamidino-2-phenylindole (DAPI) staining. The covering of the surface area of the plastic by bacterial cells was determined using Image J software. Cell enrichment factors were calculated by the ratio between bacterial counts in PMD and in the FL fraction, brought forward to a same volume of 1 mm^{-3} when considering a mean PMD thickness of 100 μm.

For qualitative assessment of biofilm structure, a random collection of 8 samples was chosen for scanning electron microscopy (SEM) using Inspect S50 (FEI, Hillsboro, OR, USA), as described previously (Zettler *et al.,* 2013). Some of the samples were also analyzed by atomic force microscope (AFM) to get more resolved insight of the surface, using a Nanoscope V in dynamic mode (Bruker instruments, Madisson, WI, USA) and standard silicon probes (Bruker, TESP-V2) (Binnig and Quate, 1986).

DNA extraction and next-generation sequencing

DNA was extracted from 72 PMD and from all the 3 μm- and 0.2 μm-pore size filters from surrounding seawater from each of the 32 stations. Between 2 and 4 plastic fragments were extracted separately at each station to evaluate intra-site variability. DNA extraction followed a classical phenol-chloroform-based protocol (Ghiglione *et al.*, 1999) with an additional sonication step (3 x 5 sec with 30% amplitude, Branson SLPe) for a better disruption of the biofilm. The molecular size and the purity of the DNA extracts were analyzed by agarose gel electrophoresis (1%) and the DNA was quantified by spectrophotometry (GeneQuant II, Pharmacia Biotech). Primers for PCR amplification of the 16S V3–V5 region were 515F-Y and 926R, particularly well-suited for marine samples according to Parada *et al*. (2016), with

Illumina-specific primers and barcodes. Sequencing was performed on an Illumina MiSeq by Research and Testing Laboratories (Lubbock, TX). Raw FASTA files were deposited at GenBank under the accession number SRP102645. Paired raw reads were joined, quality-filtered and assigned to taxa using Qiime pipelines, as previously described (Severin *et al.*, 2016). Operational taxonomic units (OTUs) were defined as clusters sharing 97 % sequence identity. Only Bacteria were treated in this study, due to the small number of Archaea reads. Bacterial sequences were randomly resampled in the OTU file to enable comparison between samples, by normalizing the number of sequences between samples to the sample with the fewest sequences (n=8,541) using MacQiime 1.9.0 (single_rarefaction.py). All further analyses were performed on the randomly re-sampled OTU table.

Statistical analysis, diversity assessment and predictive metagenome analysis

Alpha diversity was estimated by non-parametric Chao1 species richness estimator using SPADE software; together with Simpson, Shannon and Pielou diversity indexes using PRIMER 6 (PRIMER-E, UK). Differences between FL, PA and PMD richness and diversity indexes were tested using non-parametric Kruskal-Wallis test (R software). Nonmetric multidimensional scaling (NMDS) was used for visualization of beta-diversity based on Bray-Curtis similarities. One-way analysis of similarity was performed on the same distance matrix (ANOSIM, PRIMER 6) to test the significant difference and to partition the variance of the beta-diversity matrix between FL, PA and PMD. We performed a PICRUSt analysis to obtain a predictive functional profile of the bacterial communities, calculated by linking individual species to metabolic functions. The mean of Nearest Sequenced Taxon Index (NSTI) had a score of 0.08 ± 0.03, thus indicating a reliable estimation of the predictions for our samples (Langille *et al.*, 2013). We identified the OTUs or the functions primarily responsible for dissimilarities between pairs of FL, PA and PMD groups using similarity percentage analysis

(SIMPER, PRIMER 6). To investigate the relationships between bacterial community structure and environmental parameters, we used a direct multivariate gradient approach, i.e., a canonical correspondence analysis (CCA) using the software package CANOCO 4.5, as previously described (Berdjeb *et al.*, 2011). Spearman rank pairwise correlations between the environmental variables helped to determine their significance. We used a Monte Carlo permutation full model test (199 permutations) to statistically evaluate the significance of the canonical axes. Explanatory variables were determined first by using a forward-selection procedure (999 permutations) and second, by successive addition of variables until it failed to contribute significantly ($p<0.05$) to a substantial improvement of the model.

Results

PMD characterization and environmental parameters

We visually selected 80 PMD in order to get between 2 to 5 pieces for each of the 32 Manta trawls. The size, shape, color, composition and oxidation state were determined for all pieces (Suppl. Table 1). The pieces showed varied shapes like filaments, pellets or sheets with about 46% transparent, 28% white and 12.5% colored (Figure 1). Zooscan analysis showed that the pieces were on average of 9.3 mm in size (SD=4.7). Ranging from 2.8 to 23.8 mm, most of the pieces did not correspond exactly to the arbitrary limit of microplastics (size <5mm), but were representative of the majority of PMD recovered in all manta nets. The shape of the pieces, as depicted by the contour circularity, ranged between 0.05 and 0.75 (mean=0.39, SD=0.14). FTIR analysis revealed that polyethylene (PE) dominated the composition in the 80 plastic pieces (72.2%), followed by polypropylene (PP) (18.0%), polystyrene (PS) (2.8%) and others, mainly dominated by composite plastics (7.0%). The mean carboxyl index (COi) was on average 15.3% (SD=12.5%; min=1.6% and max=93.2%, both extreme values reached in PE pieces) with more than 8% of PMD presenting higher degree of oxidation (>25 %).

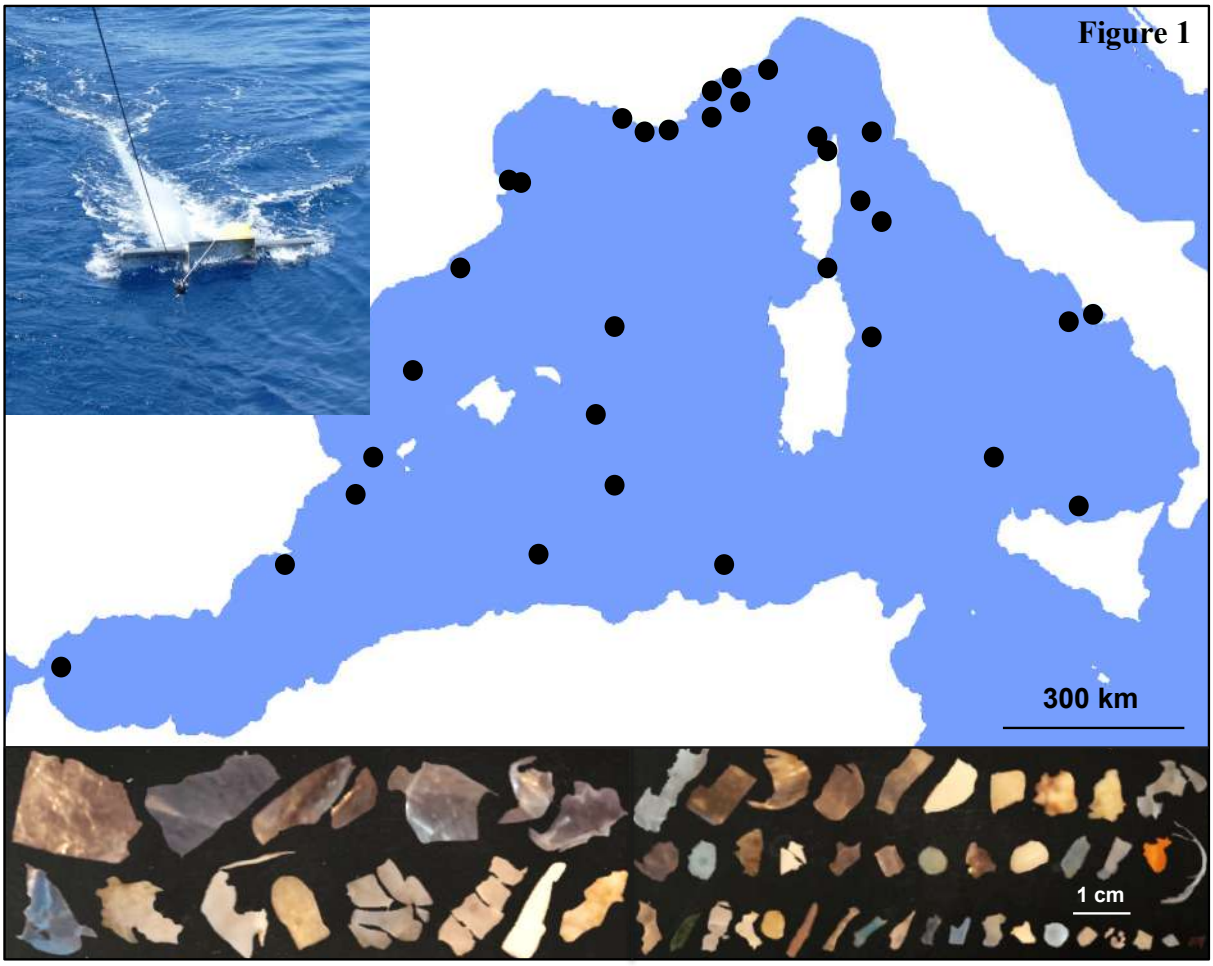

Bacterial abundance on PMD

Inspection of 72 plastic pieces from 20 manta trawls by epifluorescence microscopy revealed that most of the samples were highly colonized by bacteria (Figure 2). Bacterial counts were on average 4.4×10^4 cells mm^{-2} (SD = 3.7×10^3). It corresponded to an average enrichment factor of 888 (SD = 731, min=80 and max=3748) compared to the FL bacteria in surrounding waters, when considering the same volume. Variation in cell density (between 1.1×10^3 and 1.9×10^5 cells mm^{-2}) could not be statistically correlated to PMD characteristics (surface, shape) or environmental parameters (distance to the coast, temperature, salinity and chlorophyll *a* of the surrounding water). A large variety of morphotype was observed (Figure 2), including coccus-, rod- and spiral-shaped cells with a large number of cells with

prosthecae and long filaments together with cells with pili and flagella. We often observed Cyanobacteria, such as *Calothrix sp.* frequently embedded in an amorphous mass of *Pleurocapsa sp.* cells. Often occurring in rows or patches, bacteria were non-uniformly distributed on the plastic surface, covering between 0 and 3.5% of the surface area of the plastic. Other eukaryotic organisms were observed on plastics, mainly diatoms and more randomly dinoflagellates, fungi and bryozoans, but were not further considered in this study. All plastics showed signs of degradation, including cracks and pitting hosting numerous organisms, as shown by scanning electron microscopy (SEM) and atomic force microscopy (AFM) (Figure 2).

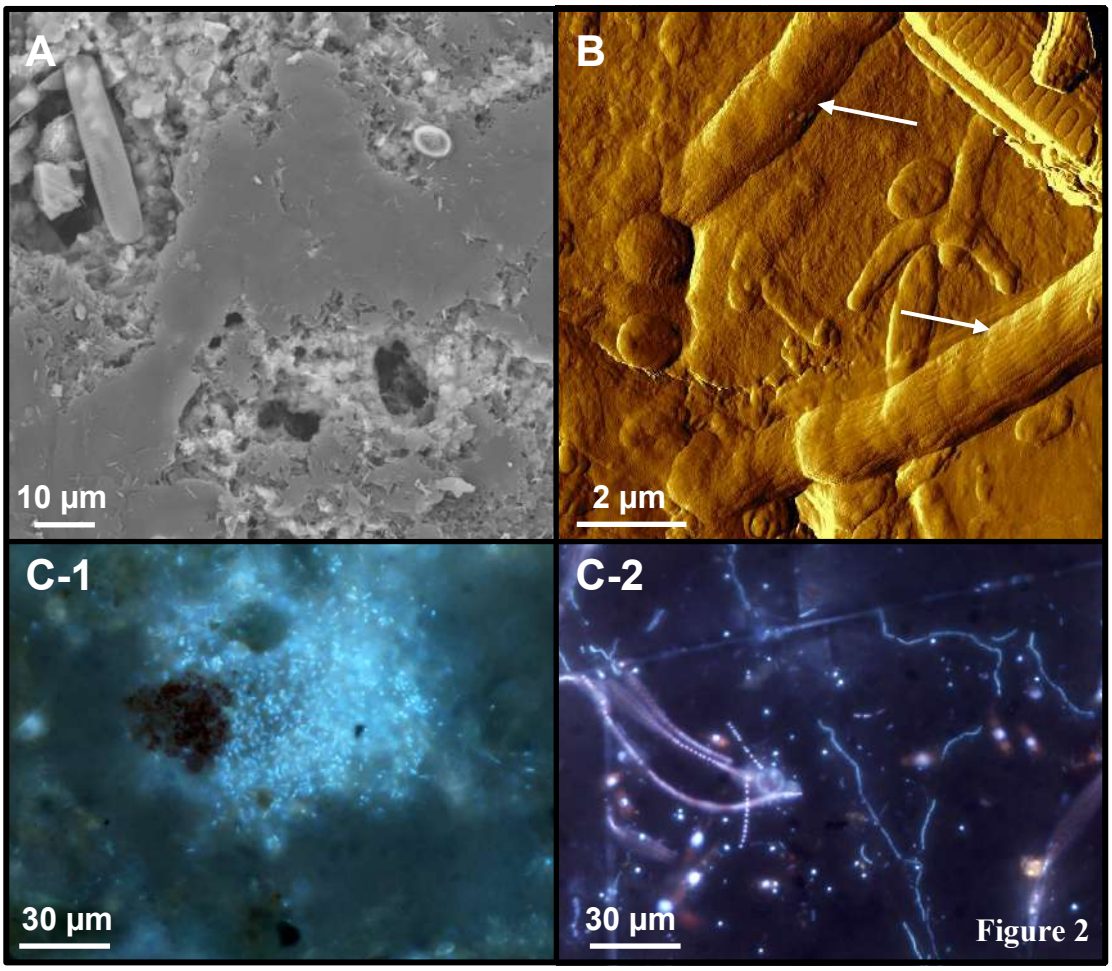

Figure 2

Diversity indexes of PMD colonizers compared to FL and PA fractions

Next-generation DNA sequencing resulted in 1,135,953 sequences tags falling into 1,340

OTUs at the 97% similarity level, after randomly resampling to 8,541 sequences per sample to provide statistical robustness when comparing diversity measures among samples. Each of the FL, PA and PMD fractions were composed of 35.1, 56.0 and 83.6% of the total number of OTUs, respectively. Rarefaction analysis (not shown) suggested that the FL, PA and PMD bacterial diversity approached that of an asymptote. Chao1 estimator showed that the richness of the PA (mean=173, SD= 41.7, n= 24) was significantly higher (Kruskal-Wallis test, $p<0.001$) than the FL community (mean=125, SD=39.5, n=28), whereas PMD communities presented intermediate values (mean=160, SD=69.5, n=74) non-significantly different from the other two fractions (Figure 3). Pielou index revealed a significantly higher evenness in the PMD community (mean=0.65, SD=0.10) compared to the PA (mean=0.53, SD=0.11) and FL fractions (mean=0.60, SD=0.07) (Kruskal-Wallis test, $p<0.001$). Consequently, PMD presented a significantly higher Shannon diversity index (mean=3.10, SD=0.47) compared to the PA (mean=2.62, SD= 0.59) and FL fractions (mean=2.71, SD= 0.30) (ANOVA $p<0.001$).

Figure 3

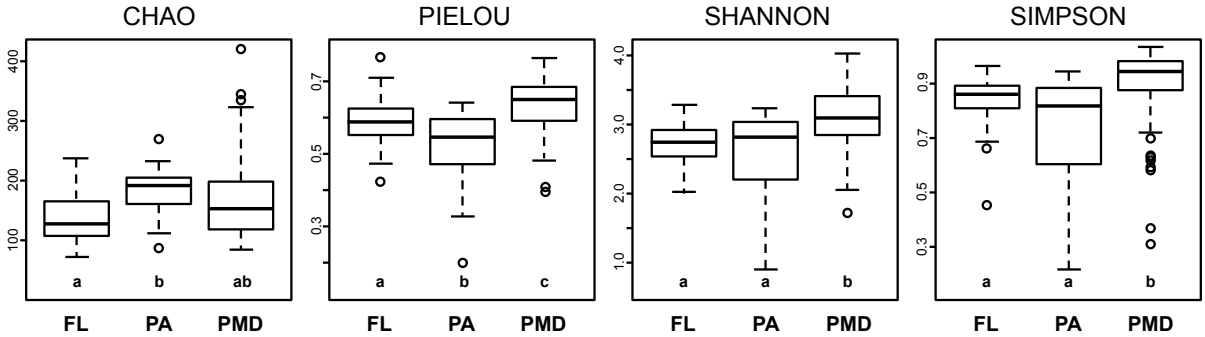

Bacterial community structure in relation to PMD characteristics and environmental parameters

Non-metric multidimensional scaling (NMDS) based on Bray–Curtis dissimilarities revealed that the global pattern of bacterial diversity was explained in part by the FL, PA and PMD lifestyles (Figure 4). Analysis of similarity (ANOSIM) showed these groups to be highly significant (UniFrac and p test significance, both $p<0.001$). The overall dissimilarity between

PMD cluster and FL and PA cluster was 69%. FL and PA formed distinct sub-clusters with lower within dissimilarities than in the PMD cluster (41, 52 and 60%, respectively). To evaluate the factors driving the bacterial community structure of the PMD communities, we performed a canonical correspondence analysis (CCA) (Suppl. Figure S1). The best statistical model explained only 11.0% of the total variance ($P < 0.05$). Variation partitioning indicated that the PMD characteristics (surface, shape and carbonyl index) and the few environmental variables available across all datasets (temperature, salinity and Chl *a*) contributed equally to the total variance explained. No significant relationship was found neither with the polymer type (i.e. PE, PP, PS and others) nor among the geographical sampling sites (inter-site) or within plastic pieces sampled in the same Manta trawl (intra-site).

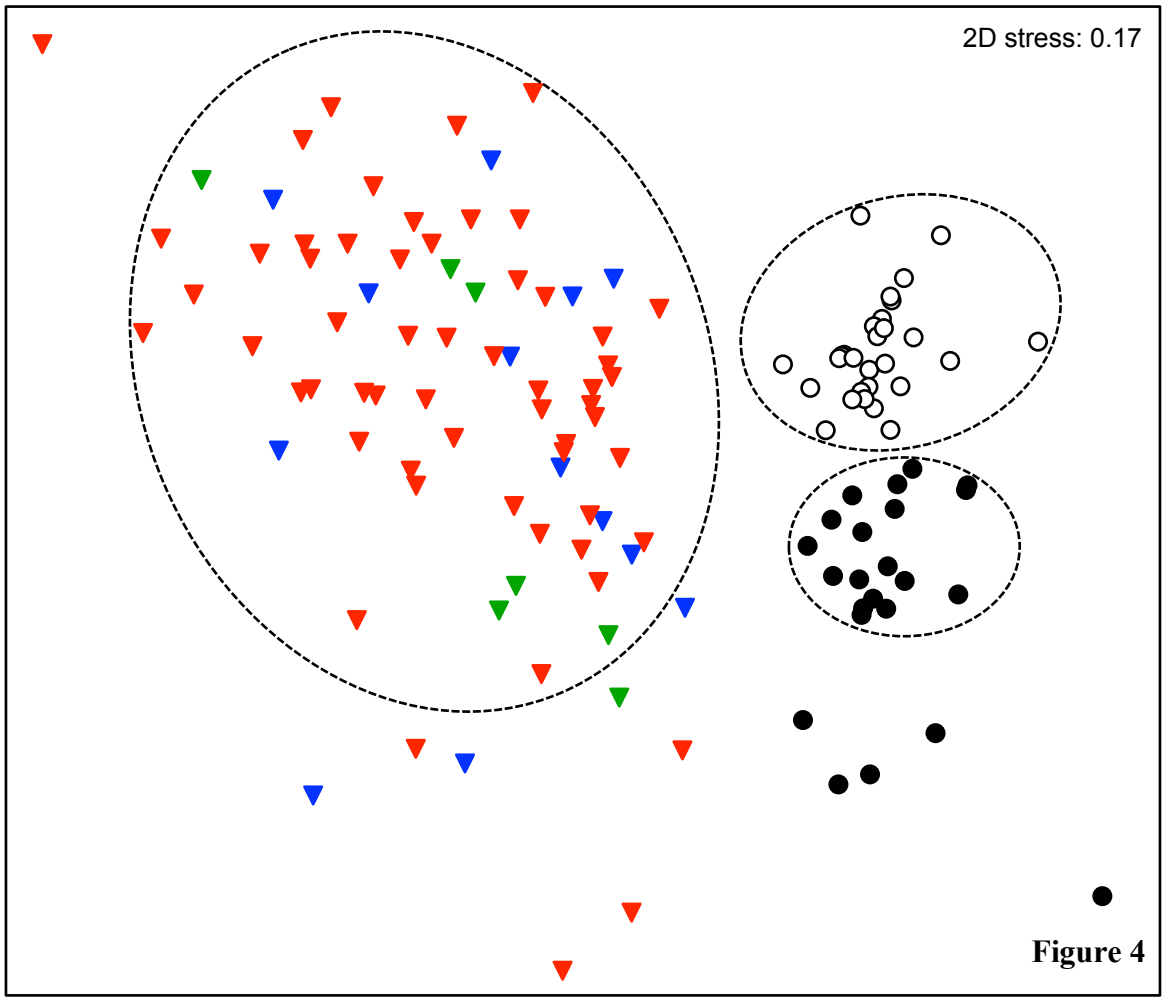

Figure 4

Taxonomic difference between FL, PA and PMD fractions

Most of the OTUs in the FL fraction were dominated by Alphaproteobacteria (45.0%, mainly *Pelagibacter sp.*), followed by Cyanobacteria (24.3%, mainly *Synechococcus sp.*), Flavobacteria and Gammaproteobacteria (11.3% and 11.1%, respectively) (Figure 5). OTUs in the PA fraction were characterized by closer percentages between the 3 dominant classes, including Alphaproteobacteria (25.9%, mainly *Erythrobacter sp.*), Gammaproteobacteria (25.0%, mainly *Alteromonas sp.*) and Cyanobacteria (17.9%, mainly *Synechococcus sp.*). The PMD fraction was dominated by Cyanobacteria (40.8%, mainly *Pleurocapsa sp.*) and Alphaproteobacteria (32.2%, mainly *Roseobacter sp.*). Most of the Cyanobacteria belong to Oscillatoriales, Chroococcales, Nostocales and Pleurocapsales orders. *Synechococcus sp., Calothrix sp., Scytonema sp.* and *Pleurocapsa sp.* were the more represented species.

Venn diagram revealed a large fraction (46.7%, dominated by *Ulvibacter litoralis*, *Rivularia sp., Microchaete tenera* and *Shimia marina*) of the total OTUs found only in the PMD fraction. A very small fraction (5.9%, dominated by Marinimicrobia) was found only in FL, whereas specific OTUs found in PA represented 15.3% (dominated by Vibrionaceae). The ubiquitous OTUs found in the three fractions represented 24.6% (Figure 6).

Similarity percentage analysis (SIMPER) revealed 12 individual OTUs contributing to 50% of the dissimilarity between PMD and the surrounding water, including *Pleurocapsa sp., Calothrix sp., Scytonema sp.* and Oscillatoriales more abundant in the PMD and *Synechococcus sp*., *Pelagibacter sp*., *Alteromonas sp*. more abundant in FL and PA fractions (Figure 7). Comparison between PA and FL showed that five OTUs contributed to 50% of the dissimilarity, including *Pelagibacter sp.* and *Synechococcus sp*. more represented in FL and *Alteromonas sp.* more abundant in PA.

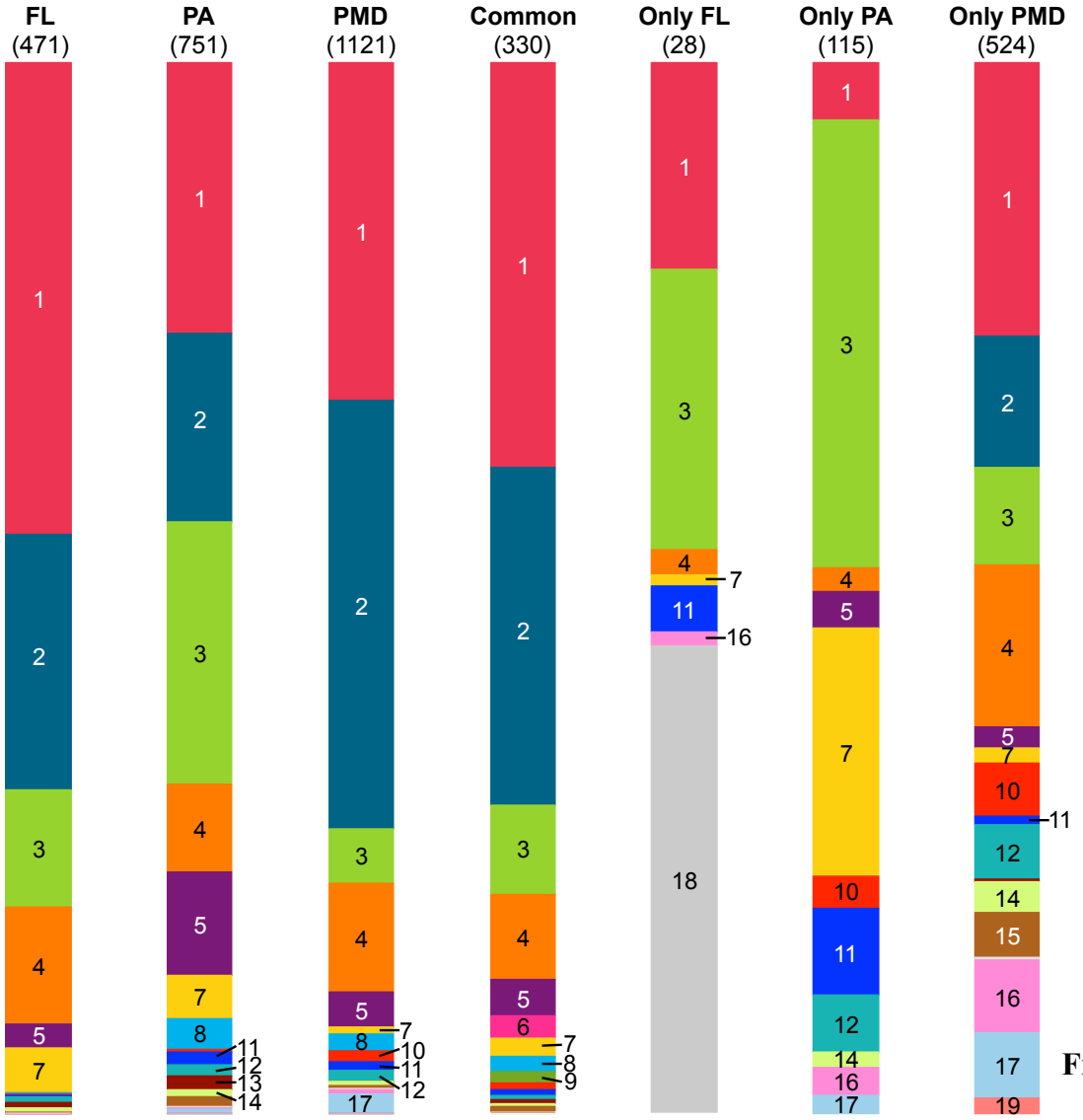

Figure 5

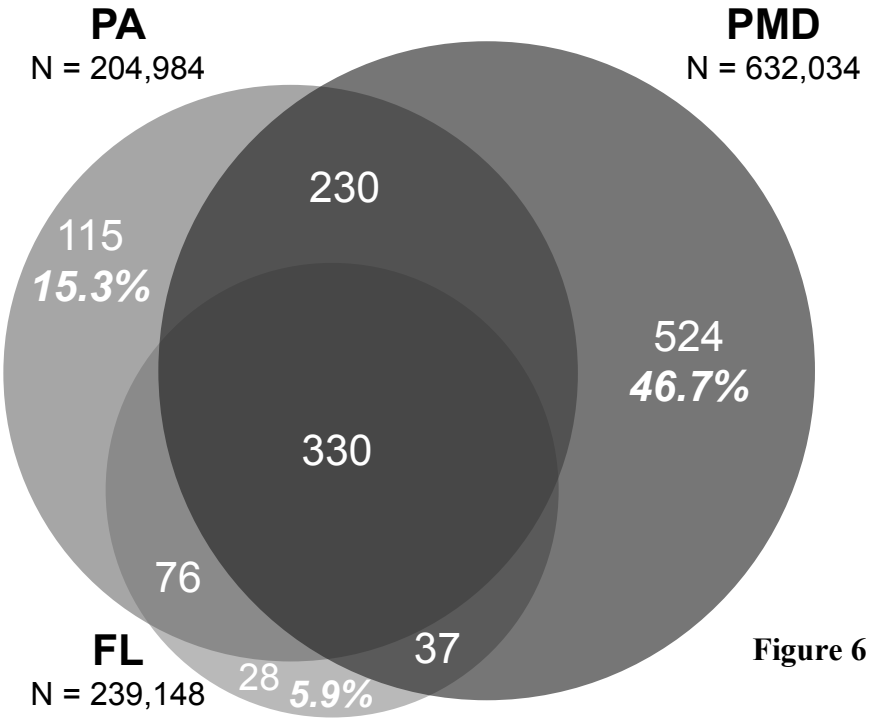

Figure 6

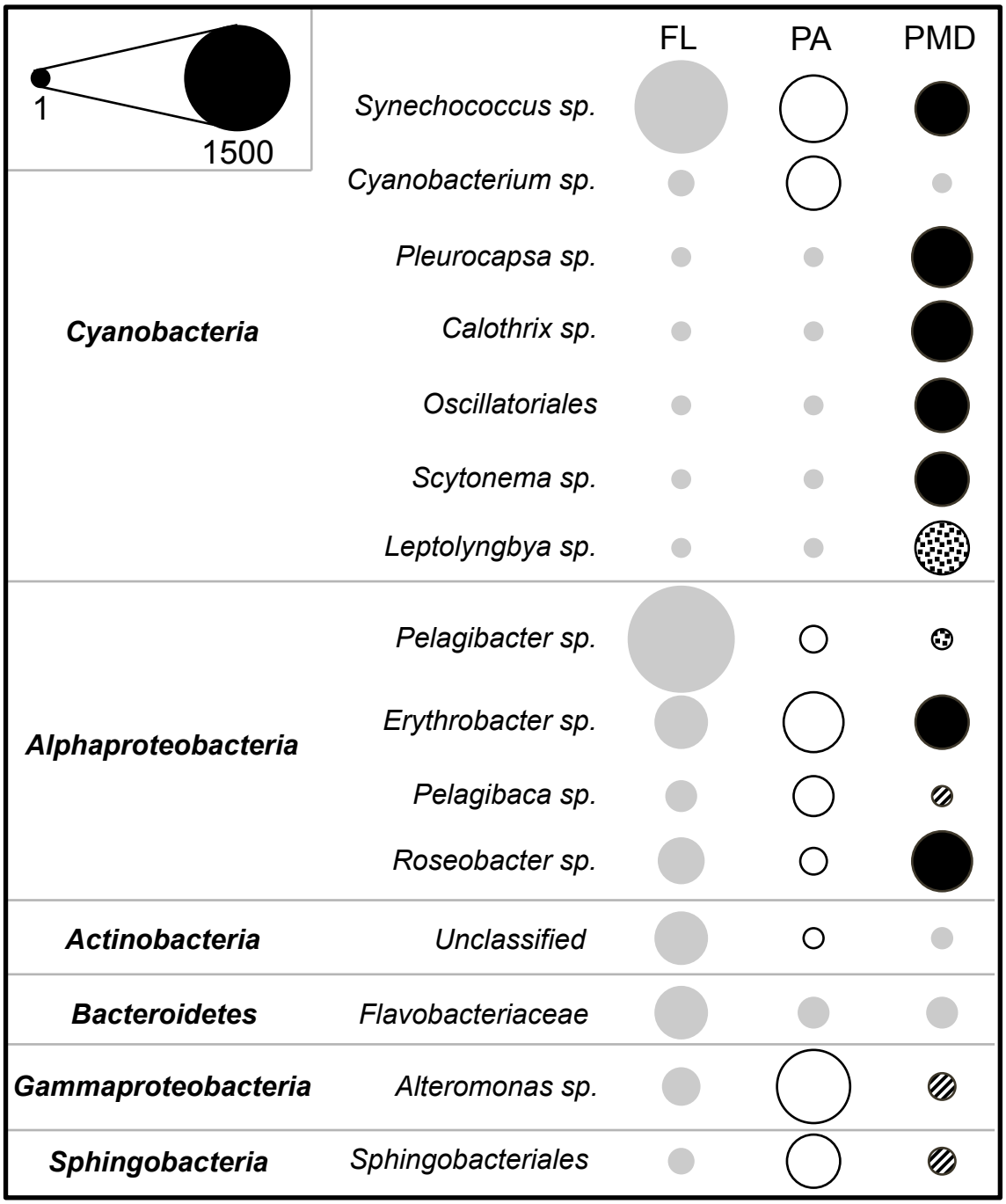

Figure 7

Potential metabolic differences between bacteria in FL, PA and PMD fractions

Analysis of the predicted metabolic functions potentially expressed by the bacterial communities associated to FL, PA and PMD fractions revealed several systematic differences (Figure 8). On KEGG level 2 (high hierarchical level in PICRUSt), membrane transport, cell motility and xenobiotics biodegradation were predicted to be significantly more encoded by PMD compared to FL communities (Kruskal-Wallis rank sum test; $p<0.05$), while KEGG

terms related to translation, replication and repair and amino acid metabolism were predicted to be more represented in the FL fraction. We further used SIMPER to discriminate the predictive functions at a lower hierarchical level (KEGG level 3) explaining the most differences between the 3 fractions (the 20 most abundant functions contributing to 36.7% difference). General transporters and ABC transporters functions were more detected on PMD and explained from 10.5 to 13.8% of the dissimilarity with FL and PA. Xenobiotic biodegradation and metabolism functions were also more found on PMD. Photosynthesis proteins, cell motility, cellular process and signaling were more represented in both PMD and PA compared to FL.

Figure 8

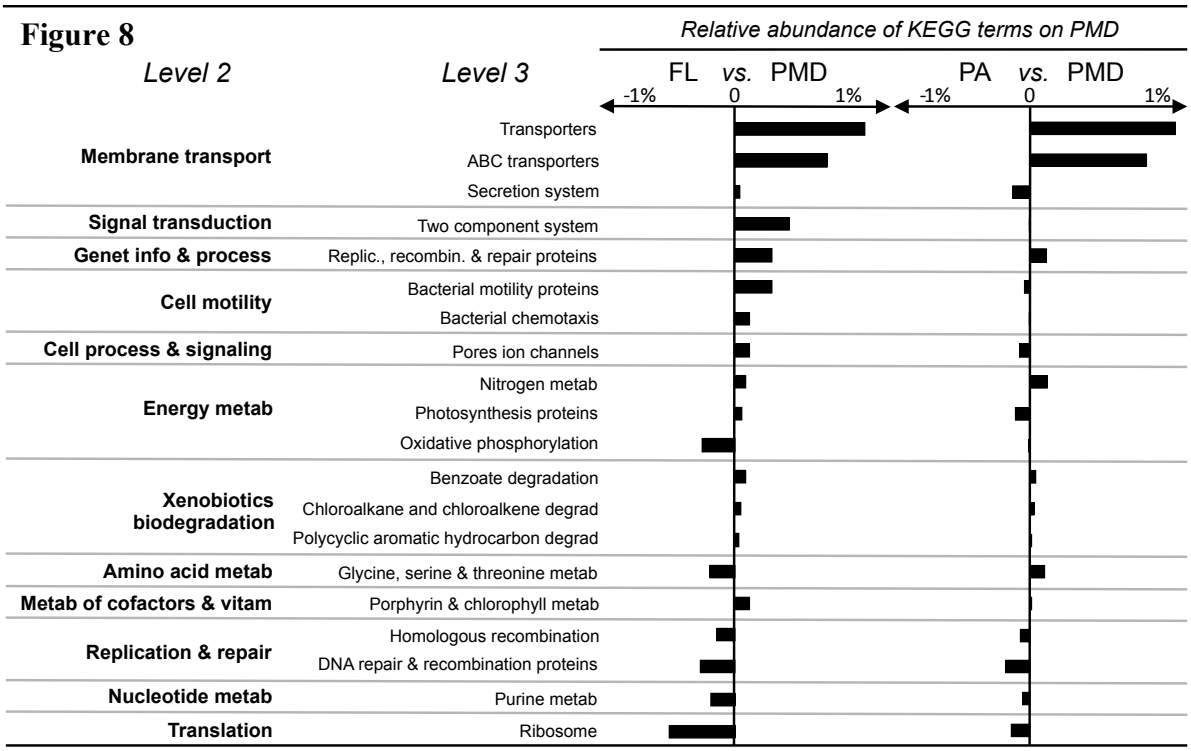

A closer look at the OTU table for known hydrocarbonoclastic bacteria (77 OTUs including *Glaciecola sp., Muricauda sp., Pseudoalteromonas sp., Hyphomonas sp., Phormidium sp., and Erythrobacter sp.,* which represented generally more than 0.1% of the community for each sample) showed that these OTUs were more present in PMD and PA fractions (7.4 and 7.8%, respectively) compared to FL (4.7%). The most dominant hydrocarbonoclastic OTUs

was *Erythrobacter sp.,* which dominated some samples of the PMD (43%) and PA (35%) communities. *Hyphomonas sp.* and *Phormidium sp*. in particular were 10 to 100 times more found in PMD compared to PA and FL, and were observed in almost all the plastic pieces.

We also focused on putative pathogens, based on taxonomic OTU identification. *Vibrio sp.* was generally found in the rare biosphere (<0.1%) in the FL, and sometimes in higher proportion in PMD and PA. Putative pathogen *Vibrio* species such as *V. anguillarum, V. harveyi, V. pectenicida* and *V. xiamenensis* were found on less than 5 plastic pieces, and neither detected on FL and PA. Other putative pathogens were particularly found on PMD and rather rare in PA and FL, such as the fish pathogen *Tenacibaculum sp.* or the crustacean and invertebrate pathogens *Phormidium sp.* and *Leptolyngbya sp.,* which were observed in more than three quarters of plastic pieces and represented 27.7% of the PMD community.

Discussion

A high density but patchy distribution of bacteria living on PMD compared to the PA and FL lifestyles.

We found a very high density of bacteria living on plastics, with a mean of 4.4×10^4 cells mm^{-2}. This is in the same order of magnitude as found in seawater biofilms covering glass (Mieszkin *et al.*, 2012), subtidal rocks (Chung *et al.*, 2010) or stainless steel (Devi, 1995). Microplastic concentration ranged between <1 to 36 pieces m^{-3} in the surface layers of the North Western Mediterranean Sea (Pedrotti *et al.*, 2016; Collignon *et al.*, 2012), thus suggesting that microplastics can no longer be considered as a negligible part of the marine particles in this region. Our epifluorescence microscopic observations give the first *in situ* estimation of the bacterial density on PMD in marine waters, even if plastic biofilms have been observed by electron microscopy in a number of studies starting in the 1970s (Carpenter *et al.*, 1972). We found that PMD cell enrichment factor (EF) was up to 4000 and more

generally around 900 compared to FL fraction, which is similar and even higher to EF generally observed for PA bacteria (Simon *et al.*, 2002). The biofilms covered between 0 and 3.5% of the surface area, revealing a rather patchy and non-uniform covering of the PMD. This observation is in accordance with the *in situ* observation of spatial heterogeneity ('patchiness') of mature biofilms in nature, controlled by a complex set of parameters including physical (hydrodynamic fluxes), chemical (nutrients, pH, oxygen) and biological conditions (quorum-sensing, toxic metabolic by-products) (Flemming *et al.*, 2016; Salta *et al.*, 2013).

PMD bacteria presented similar richness but higher evenness compared to FL and PA

We observed that PMD represent favorable environments for a large number of species, with significantly higher evenness compared to FL and PA fractions. These results are in accordance with Zettler et al. (2013), but differed with Mc Cormick et al. (2014), both comparing PMD and FL communities only. Such discrepancy may be due to the low number of samples analyzed in the previous studies (3 and 4 sites with a total of 6 and 4 PMD, respectively) compared to the 32 sites and 80 PMD analyzed here, which make the conclusions more robust. Theoretical studies suggested that spatial isolation (such as the colonization of PMD in seawater in our case) could limit competition, thereby supporting a high richness and a more uniform diversity (Zhou *et al.*, 2002). Further studies are needed to test if this trend may be explained by the superabundant or heterogeneous resources, fluctuating conditions and spatial heterogeneity offered by PMD.

Niche partitioning between PMD, FL and PA fractions.

NMDS results demonstrated niche partitioning in marine bacteria as reflected by the considerable proportion of the variance (69%) in community composition between PMD and

the surrounding FL or PA fractions. Niche partitioning is one of the hypotheses that could explain the maintenance of the tremendous diversity among marine bacteria, together with their capacity for dormancy (Baran *et al.*, 2015). The classical barriers known to affect the pelagic bacterial communities are transitions between marine and freshwater, coast and offshore or surface and deep waters (Ghiglione *et al.*, 2012). Here, we propose that spatial isolation provided by the large concentration of PMD offer a distinct strategy to avoid competition by occupying different physical locations, which support a new trade-off for the maintenance of a large diversity of bacteria in the Oceans (Sunagawa *et al.*, 2015). Together with additional metabolic diversification of sympatric microbial populations (i.e., resource limitation and cross-feeding), the evidence of spatial isolation on PMD give a new example of bacterial strategy to explain the high diversity of pelagic microbes in the Oceans, analogous to the "Hutchinson's paradox of the plankton" for phytoplankton (Hutchinson, 1961).

Transition from one lifestyle to another and niche specificities.

Over the thousands of OTUs identified, a quarter of them were 'generalists'. It suggests possible exchanges between the PMD, PA and FL communities rather than considering the three compartments as non-interacting environments. Attachment and detachment is a common feature already observed in biofilms and organic particles, with release of cells that become free, return to the planktonic mode of growth until they encounter another physical carrier (Stoodley *et al.*, 2002; Ghiglione *et al.*, 2007).

Interestingly, we observed that OTUs only found on PMD represented almost half of the total OTUs in our samples, thus suggesting a distinct selection strategy and reinforcing the view of PMD being a particular biota for marine bacteria. We may have hypothesis a high similarity between OTUs living on PMD and PA, as previously suggested in one study focusing on the early colonization of polyethylene terephthalate (PET) bottles in seawater (Oberbeckmann et

al. 2016). It was not the case in our study, with more than half of OTUs being distinct between these very different PA and PMD habitats. PA bacteria decompose the support where they live, which is made of detritus-dominated aggregates sinking in the water column (Simon *et al.*, 2002). This is not the case for PMD that presented very low biodegradation rates (Dussud and Ghiglione, 2014). Floating PMD are different habitats, with a longer history of drifting dispersion and being periodically submitted to ultraviolet (UV) radiation, mechanical forces and weathering, as well as to ingestion and release by pelagic filter feeders, and other zooplankton and micronekton (Collignon *et al.*, 2012).

Finally, we observed that 'FL specialists' were rather an exception than a rule, since the OTUs found exclusively in a FL state represented less than 6%. Similar tendency was found when comparing only FL and PA communities, using similar metabarcoding approach (Rieck *et al.*, 2015). Our results reinforce the view of Grossart et al. (2010), who underlined that much less attention has been paid to the large diversity of bacteria living on PMD and PA compared to FL, which may influence in an erroneous way emerging concepts in marine microbial ecology.

Taxonomic identification and predictive functions.

Bacteria living on PMD were dominated by Cyanobacteria and Alphaproteobacteria, whereas FL and PA fractions were in line with the general trends previously observed, i.e. with the FL dominated by Alphaproteobacteria (mainly *Pelagibacter sp.*) and PA dominated by Alphaproteobacteria (mainly *Erythrobacter sp.*) and Gammaproteobacteria (mainly *Alteromonas sp.*) (Crespo *et al.*, 2013; Mohit *et al.*, 2014). Consistent with the typical Cyanobacteria shapes widely observed in our SEM and AFM images, SIMPER analysis revealed that most of the taxonomic groups explaining the difference between the PMD vs. PA and FL belong to this group. It confirmed the specific occurrence of some OTUs in PMD

biofilms, where the presence of light and inorganic carbon released by neighbor microorganisms may be a driving factor for the selection of Cyanobacteria (Stal, 1995). Five genera of Cyanobacteria were particularly more represented in the PMD, including *Leptolyngbya sp., Pleurocapsa sp.* and *Rivularia sp.*, which were already observed in the plastisphere in the North Pacific gyre (Zettler *et al.*, 2013; Bryant *et al.*, 2016). We also noted the presence of *Scytonema sp.* and *Calothrix sp.* in PMD, which were previously found on biofilms covering rocks or chalky crustaceans (Sivonen *et al.*, 2007; González-Resendiz *et al.*, 2015). Further studies are needed to evaluate the influence of the photosynthetic activities of Cyanobacteria living on PMD on the global pelagic primary production and more generally on their biogeochemical role on the carbon and nitrogen cycles in the Oceans.

In parallel, we used our OTU table for the prediction of microbial metagenomes, as recently proposed by several authors (Langille *et al.*, 2013; Louca *et al.*, 2016). PICRUSt analysis highlighted the dominance of porphyrin and chlorophyll metabolism functions on the PMD compared to FL and PA genomes. Although these observations were based only on predictions made from 16S rRNA gene sequences, this is consistent with the metagenomic data obtained from 12 plastic pieces in the North Pacific Gyre (Bryant *et al.*, 2016). Other prediction of overrepresented functional categories on PMD compared to FL and PA were also plausible: the membrane transport functions and the ABC transporters, as well as the cellular processes and signaling were previously described as essential functions in biofilm formation and maturation (Lasa and Penadés, 2006; Porter *et al.*, 2011; He and Bauer, 2014); the cell motility was described as a prerequisite for the chemotactic behavior and active interactions between bacteria and colonization sites (Simon *et al.*, 2002). Even though the overrepresentation of some functional categories needs to be interpreted with caution, this predictive method provided a good indication for the existence of functional differences in our system.

Evidence of bacterial degradation of hydrocarbon-based PMD remains an unresolved hypothesis in marine waters (Dussud and Ghiglione, 2014). Interestingly, several hydrocarbonoclastic bacteria were overrepresented in the PMD fraction, such as Erythrobacteraceae (e.g. *Erythrobacter sp., Croceicoccus naphtovorans*) (Wang *et al.*, 2016) or *Hyphomonas sp.* (Li *et al.*, 2014) found in almost all our plastic pieces. Predicted genomes of bacteria predominantly found in PMD were also notably enriched in xenobiotics biodegradation functions, mainly including hydrocarbon degradation. However, further investigations are needed to evaluate how much these consortia are good candidates for PMD biodegradation, since they may also be selected by hydrocarbon petroleum residues concentrated on their surfaces due to the hydrophobic properties of PMD (Rios *et al.*, 2007).

Interests have been raised about opportunist pathogens dispersal on PMD, such as animal or human pathogenic *Vibrio sp.* (Zettler *et al.*, 2013). The potentially human pathogenic *Vibrio parahaemolyticus* was recently observed on a number of PMD from North/Baltic Sea (Kirstein *et al.*, 2016), but were never detected in our dataset. Other potentially pathogenic *Vibrios* were observed, such as *V. anguillarum, V. harveyi, V. pectinicida, V. xiamenensis*, but they generally belong to the rare biosphere (<0.1%) and they were not related to human diseases. Overall, *Vibrio* sp. was 7 times higher in the PMD compared to FL, but they were not particularly enriched compared to the PA fraction. SIMPER analysis highlighted the overrepresentation of *Tenacibaculum sp.*, *Phormidium sp.* and *Leptolyngbya sp.* in the PMD compared to both FL and PA, a few members of these genus being known as fish pathogens (Austin *et al.*, 2012) or brine shrimp and coral black band disease (Rützler and Santavy, 1983; Frazão *et al.*, 2010). However, caution should be taken since metabarcoding approach is not an appropriate method for describing bacterial virulence, and further tests are needed before waving alarmist conclusions on the potential role of PMD as vector for the dispersal of harmful or even human pathogenic species (Kirstein *et al.*, 2016).

Conclusion

This study successfully evidences the occurrence of a specific and abundant bacterial life on PMD, when compared to the more frequently studied FL and PA fractions in the surrounding waters. Such niche partitioning raised stimulating questions about the functional role of these abundant communities, which are increasing together with the number of PMD in the World Ocean. Based on a large set of samples along the western Mediterranean Sea, our study gives new directions to estimate the ecological role of PMD communities, and in particular the Cyanobacteria group consistently found abundant on PMD that may influence the global carbon and nitrogen biogeochemical cycles in surface Oceans. Computational predictions also gave evidence of specific functions associated to PMD such as hydrocarbon degradation, which needs further studies to evaluate their capability to perform plastic biodegradation in marine waters.

Acknowledgements. *We thank the commitment of the following institutions, people and sponsors: CNRS, UPMC, LOV, Genoscope/CEA, the Tara Expeditions Foundation and its funders: agnès b. and Etienne Bourgois, the Veolia Environment Foundation, Lorient Agglomeration, Serge Ferrari, the Foundation Prince Albert II de Monaco, IDEC, the Tara schooner and teams. We are also grateful to the French Ministry of Foreign Affairs for supporting the expedition and to the countries that graciously granted sampling permissions. We thank Guigui PA, VJS, and Alburquerque N for insightful comments on the manuscript. This work was also supported by the PLASTICMICRO project founded by CNRS-EC2CO-Microbien.*

Conflict of interest. *All of the reported work is original research, and authors have seen and approved the final version submitted. The material has not been previously published and has not been submitted for publication elsewhere while under consideration. The authors declare no conflict of interest. Likewise, consent is given for publication in The ISME Journal, if accepted.*

Supplementary information. *Supplementary information is available at Environmental Pollution website.*

References

Andrady AL. (2011). Microplastics in the marine environment. *Mar Pollut Bull* **62**: 1596–605.

Austin B, Austin DA, Austin B, Austin DA. (2012). Bacterial fish pathogens. In: *Heidelberg Germany: Springer*. p 652.

Baran R, Brodie EL, Mayberry-Lewis J, Hummel E, Da Rocha UN, Chakraborty R, *et al.* (2015). Exometabolite niche partitioning among sympatric soil bacteria. *Nat Commun* **6**: 8289.

Berdjeb L, Ghiglione JF, Jacquet S. (2011). Bottom-up versus top-down control of hypo-and epilimnion free-living bacterial community structures in two neighboring freshwater lakes. *Appl Environ Microbiol* **77**: 3591–3599.

Binnig G, Quate CF. (1986). Atomic Force Microscope. *Phys Rev Lett* **56**: 930–933.

Bryant JA, Clemente TM, Viviani DA, Fong AA, Thomas KA, Kemp P, *et al.* (2016). Diversity and Activity of Communities Inhabiting Plastic Debris in the North Pacific Gyre. *mSystems* **1**: e00024-16.

Carpenter E, Anderson S, Harvey G, Miklas H. (1972). Polystyrene spherules in coastal waters. *Science* **178**: 749–750.

Chung HC, Lee OO, Huang Y-L, Mok SY, Kolter R, Qian P-Y. (2010). Bacterial community succession and chemical profiles of subtidal biofilms in relation to larval settlement of the polychaete Hydroides elegans. *ISME J* **4**: 817–828.

Collignon A, Hecq J-H, Glagani F, Voisin P, Collard F, Goffart A. (2012). Neustonic microplastic and zooplankton in the North Western Mediterranean Sea. *Mar Pollut Bull* **64**: 861–864.

Cózar A, Echevarría F, González-Gordillo JI, Irigoien X, Ubeda B, Hernández-León S, *et al.* (2014). Plastic debris in the open ocean. *Proc Natl Acad Sci* **111**: 10239–10244.

Crespo BG, Pommier T, Fernández-Gómez B, Pedrós-Alió C. (2013). Taxonomic composition of the particle-attached and free-living bacterial assemblages in the Northwest Mediterranean Sea analyzed by pyrosequencing of the 16S rRNA. *Microbiol Open* **2**: 541–552.

Devi P. (1995). Abundance of bacterial and diatom fouling on various surfaces. *Proceeding-Indian Natl Sci Acad* **61**: 231–231.

Durrieu de Madron X, Guieu C, Sempéré R, Conan P, Cossa D, D'Ortenzio F, *et al.* (2011). Marine ecosystems' responses to climatic and anthropogenic forcings in the Mediterranean. *Prog Oceanogr* **91**: 97–166.

Dussud C, Ghiglione JF. (2014). Bacterial degradation of synthetic plastics. In: Briand F (ed) Vol. 46. *Marine litter in the Mediterranean and Black Seas*. CIESM Publisher: Monaco, pp 43–48.

Eriksen M, Lebreton LCM, Carson HS, Thiel M, Moore CJ, Borerro JC, *et al.* (2014). Plastic Pollution in the World's Oceans: More than 5 Trillion Plastic Pieces Weighing over 250,000 Tons Afloat at Sea. *PLoS One* **9**: 1–15.

Farooq A, Malfatti F. (2007). Microbial structuring of marine ecosystems. *Nat Rev Microbiol* **5**: 782–791.

Flemming H-C, Wingender J, Szewzyk U, Steinberg P, Rice SA, Kjelleberg S. (2016). Biofilms: an emergent form of bacterial life. *Nat Rev Microbiol* **14**: 563–575.

Frazão B, Martins R, Vasconcelos V. (2010). Are known cyanotoxins involved in the toxicity of picoplanktonic and filamentous north atlantic marine cyanobacteria? *Mar Drugs* **8**: 1908–1919.

Gasol JM, Pinhassi J, Alonso-Sáez L, Ducklow H, Herndl GJ, Koblížek M, *et al.* (2008). Towards a better understanding of microbial carbon flux in the sea. *Aquat Microb*

Ecol **53**: 21–38.
Ghiglione JF, Conan P, Pujo-Pay M. (2009). Diversity of total and active free-living vs. particle-attached bacteria in the euphotic zone of the NW Mediterranean Sea. *FEMS Microbiol Lett* **299**: 9–21.
Ghiglione JF, Galand PE, Pommier T, Pedros-Alio C, Maas EW, Bakker K, *et al.* (2012). Pole-to- pole biogeography of surface and deep marine bacterial communities. *Proc Natl Acad Sci USA* **109**: 17633–17638.
Ghiglione JF, Mevel G, Pujo-Pay M, Mousseau L, Lebaron P, Goutx M. (2007). Diel and seasonal variations in abundance, activity, and community structure of particle-attached and free-living bacteria in NW Mediterranean Sea. *Microb Ecol* **54**: 217–231.
Ghiglione JF, Philippot L, Normand P, Lensi R, Potier P. (1999). Disruption of narG, the gene encoding the catalytic subunit of respiratory nitrate reductase, also affects nitrite respiration in Pseudomonas fluorescens YT101. *J Bacteriol* **181**: 5099–5102.
González-Resendiz L, León-Tejera HP, Gold-Morgan M. (2015). Morphological diversity of benthic nostocales (Cyanoprokaryota/cyanobacteria) from the tropical rocky shores of Huatulco region, Oaxaca, Mexico. *Phytotaxa* **219**: 221–232.
Gorsky G, Ohman MD, Picheral M, Gasparini S, Stemmann L, Romagnan JB, *et al.* (2010). Digital zooplankton image analysis using the ZooScan integrated system. *J Plankton Res* **32**: 285–303.
Gregory MR. (2009). Environmental implications of plastic debris in marine settings entanglement, ingestion, smothering, hangers-on, hitch-hiking and alien invasions. *Philos Trans R Soc Lond B Biol Sci* **364**: 2013–2025.
Grossart HP. (2010). Ecological consequences of bacterioplankton lifestyles: Changes in concepts are needed. *Environ Microbiol Rep* **2**: 706–714.
He K, Bauer CE. (2014). Chemosensory signaling systems that control bacterial survival. *Trends Microbiol* **22**: 389–398.
Hutchinson GE. (1961). The paradox of the plankton. *Am Nat* **95**: 137–145.
Kirstein I V., Kirmizi S, Wichels A, Garin-Fernandez A, Erler R, Löder M, *et al.* (2016). Dangerous hitchhikers? Evidence for potentially pathogenic Vibrio spp. on microplastic particles. *Mar Environ Res* **120**: 1–8.
Langille M, Zaneveld J, Caporaso JG, McDonald D, Knights D, Reyes J, *et al.* (2013). Predictive functional profiling of microbial communities using 16S rRNA marker gene sequences. *Nat Biotechnol* **31**: 814–21.
Lasa I, Penadés JR. (2006). Bap: A family of surface proteins involved in biofilm formation. *Res Microbiol* **157**: 99–107.
Law KL, Thompson RC. (2014). Microplastics in the seas. *Science* **345**: 144–145.
Lebreton LCM, Greer SD, Borrero JC. (2012). Numerical modelling of floating debris in the world's oceans. *Mar Pollut Bull* **64**: 653–661.
Li C, Lai Q, Li G, Liu Y, Sun F, Shao Z. (2014). Multilocus sequence analysis for the assessment of phylogenetic diversity and biogeography in Hyphomonas bacteria from diverse marine environments. *PLoS One* **9**: e101394.
Lobelle D, Cunliffe M. (2011). Early microbial biofilm formation on marine plastic debris. *Mar Pollut Bull* **62**: 197–200.
Louca S, Parfrey LW, Doebeli M. (2016). Decoupling function and taxonomy in the global ocean microbiome. *Science* **353**: 1272–1277.
McCormick A, Hoellein TJ, Mason SA, Schluep J, Kelly JJ. (2014). Microplastic is an abundant and distinct microbial habitat in an urban river. *Environ Sci Technol* **48**: 11863–11871.
Mével G, Vernet M, Goutx M, Ghiglione JF. (2008). Seasonal to hour variation scales in abundance and production of total and particle-attached bacteria in the open NW

Mediterranean Sea (0–1000 m). *Biogeosciences* **5**: 1573–1586.
Mieszkin S, Martin-Tanchereau P, Callow ME, Callow J a. (2012). Effect of bacterial biofilms formed on fouling-release coatings from natural seawater and Cobetia marina, on the adhesion of two marine algae. *Biofouling* **28**: 953–68.
Mohit V, Archambault P, Toupoint N, Lovejoy C. (2014). Phylogenetic differences in attached and free-living bacterial communities in a temperate coastal lagoon during summer, revealed via high-throughput 16S rRNA gene sequencing. *Appl Environ Microbiol* **80**: 2071–2083.
Parada AE, Needham DM, Fuhrman JA. (2016). Every base matters: Assessing small subunit rRNA primers for marine microbiomes with mock communities, time series and global field samples. *Environ Microbiol* **18**: 1403–1414.
Pedrotti ML, Petit S, Elineau A, Bruzaud S, Crebassa JC, Dumontet B, *et al.* (2016). Changes in the floating plastic pollution of the mediterranean sea in relation to the distance to land. *PLoS One* **11**: 1–14.
Porter SL, Wadhams GH, Armitage JP. (2011). Signal processing in complex chemotaxis pathways. *Nat Rev Microbiol* **9**: 153–165.
Pulido-Villena E, Baudoux AC, Obernosterer I, Landa M, Caparros J, Catala P, *et al.* (2014). Microbial food web dynamics in response to a Saharan dust event: Results from a mesocosm study in the oligotrophic Mediterranean Sea. *Biogeosciences* **11**: 5607–5619.
Rieck A, Herlemann DPR, Jürgens K, Grossart HP. (2015). Particle-associated differ from free-living bacteria in surface waters of the baltic sea. *Front Microbiol* **6**: 1297.
Rios LM, Moore C, Jones PR. (2007). Persistent organic pollutants carried by synthetic polymers in the ocean environment. *Mar Pollut Bull* **54**: 1230–1237.
Rützler K, Santavy DL. (1983). The Black Band Disease of Atlantic Reef Corals: I. Description of the Cyanophyte Pathogen. *Mar Ecol* **4**: 301–319.
Salta M, Wharton JA, Blache Y, Stokes KR, Briand JF. (2013). Marine biofilms on artificial surfaces: Structure and dynamics. *Environ Microbiol* **15**: 2879–2893.
Selke S, Auras R, Nguyen TA, Castro Aguirre E, Cheruvathur R, Liu Y. (2015). Evaluation of biodegradation-promoting additives for plastics. *Environ Sci Technol* **49**: 3769–3777.
Severin T, Sauret C, Boutrif M, Duhaut T, Kessouri F, Oriol L, *et al.* (2016). Impact of an intense water column mixing (0-1500 m) on prokaryotic diversity and activities during an open-ocean convection event in the NW Mediterranean Sea. *Environ Microbiol* **18**: 4378–4390.
Siboni N, Lidor M, Kramarsky-Winter E, Kushmaro A. (2007). Conditioning film and initial biofilm formation on ceramics tiles in the marine environment. *FEMS Microbiol Lett* **274**: 24–29.
Simon M, Grossart HP, Schweitzer B, Ploug H. (2002). Microbial ecology of organic aggregates in aquatic ecosystems. *Aquat Microb Ecol* **28**: 175–211.
Sivonen K, Halinen K, Sihvonen LM, Koskenniemi K, Sinkko H, Rantasärkkä K, *et al.* (2007). Bacterial diversity and function in the Baltic Sea with an emphasis on cyanobacteria. *Ambio* **36**: 180–185.
Stal LJ. (1995). Physiological ecology of cyanobacteria in microbial mats and other communities. *New Phytol* **131**: 1–32.
Stoodley P, Sauer K, Davies DG, Costerton JW. (2002). Biofilms as complex differentiated communities. *Annu Rev Microbiol* **56**: 187–209.
Sunagawa S, Coelho LP, Chaffron S, Kultima JR, Labadie K, Salazar G, *et al.* (2015). Structure and function of the global ocean microbiome. *Science* **348**: 1261359.
De Tender C, Devriese LI, Haegeman A, Maes S, Ruttink T, Dawyndt P. (2015). Bacterial community profiling of plastic litter in the Belgian part of the North Sea. *Environ Sci*

Technol **49**: 9629–9638.
Wang H, Wang B, Dong W, Hu X. (2016). Co-acclimation of bacterial communities under stresses of hydrocarbons with different structures. *Sci Rep* **6**: 34588.
Zettler ER, Mincer TJ, Amaral-zettler LA. (2013). Life in the ‘ Plastisphere ’ : Microbial Communities on Plastic Marine Debris. *Environ Sci Technol* **47**: 7137–7146.
Zettler LA, Zettler ER, Slikas B, Boyd GD, Melvin DW, Morrall CE, *et al.* (2015). The biogeography of the Plastisphere: Implications for policy. *Front Ecol Environ* **13**: 541–546.
Zhou J, Xia B, Treves DS, Wu L, Marsh TL, Neill RVO, *et al.* (2002). Spatial and Resource Factors Influencing High Microbial Diversity in Soil Spatial and Resource Factors Influencing High Microbial Diversity in Soil. *Appl Environ Microbiol* **68**: 326–334.

Figure legends:

Figure 1: Study area and station locations (n=32) in the Western Mediterranean Sea. Upper left: picture of the manta trawls used to collect PMD. At the bottom: light-micrograph of PMD analyzed in this study.

Figure 2: A: SEM image showing a plastic colonized by diverse organisms and surface deterioration; B: AFM amplitude error image showing pits and cracks on a very small scale, as well as organisms of different morphologies and size, among which two *Oscillatoria* are pointed (arrows) and a diatom visible on the upper right; C: Epifluorescence microscopy images of biofilms with a "patchy" organization (C-1) and a loaded biofilm with diverse morphotypes (C-2).

Figure 3: Alpha-diversity indices (Chao1, Pielou, Shannon, Simpson) of FL, PA and PMD bacteria. The boxplots show the median (heavy horizontal line inside the boxes), the box represents the first and third quartiles and unfilled circles indicate outliers. Lowercase letters (a, b, c) denote statistically different groups ($p \leq 0.05$).

Figure 4: Nonmetric multidimensional scaling (NMDS) plot showing dissimilarities among FL (open circles), PA (solid circles) and PMD (triangles: red for polyethylene, blue for polypropylene and green for other composition). Samples were grouped according to >30% Bray-Curtis similarity threshold (dotted circles).

Figure 5: Histograms showing taxonomic composition at the class level for FL, PA and PMD fractions, as well as for unique and common OTUs between the three fractions (see also Venn

diagram Figure 6). For more clarity, the class representing < 1% are not represented. Numbers of OTUs are in parentheses. (1) Alphaproteobacteria, (2) Cyanophyceae, (3) Gammaproteobacteria, (4) Flavobacteriia, (5) Sphingobacteriia, (6) Proteobacteria (unclas), (7) Actinobacteria, (8) Planctomycetia, (9) Bacteroidetes, (10) Cytophagia, (11) Bacilli, (12) Betaproteobacteria, (13) Opitutae, (14) Deltaproteobacteria, (15) Phycisphaerae, (16) Bacteroidia, (17) Clostridia, (18) Marinimicrobia.

Figure 6: Venn diagram showing overlaps between OTUs found in FL, PA and PMD fractions. Numbers inside circles represent the number of shared OTUs. The percentage of unique OTUs found in only one fraction is also indicated. N = number of reads per fraction.

Figure 7: Average abundance of the most significant OTUs contributing to 50% (cumulative) of the dissimilarity between FL, PA and PMD fractions based on SIMPER analysis. We indicated OTUs explaining the difference between FL and PA (white bubbles), FL and PMD (dotted bubbles), PA and PMD (stripped bubbles) and both FL/PMD and PA/PMD (black bubbles).

Figure 8: KEGG categories predicted by PICRUSt (level 2 and 3) differentially represented in bacterial communities found in PMD, FL and PA fractions (discriminant KEGG terms according to SIMPER analysis). Bars represent the difference of relative abundance of a KEGG term in PMD bacterial communities compared to FL fraction (left graph) or to PA fraction (right graph). Overexpression or underexpression of a KEGG term in PMD compared to FL or PA fractions are indicated by positive and negative percentage, respectively. Abbreviation of KEGG terms: metab, metabolism; info, information; process, processing; vitam, vitamins.

Supplementary files

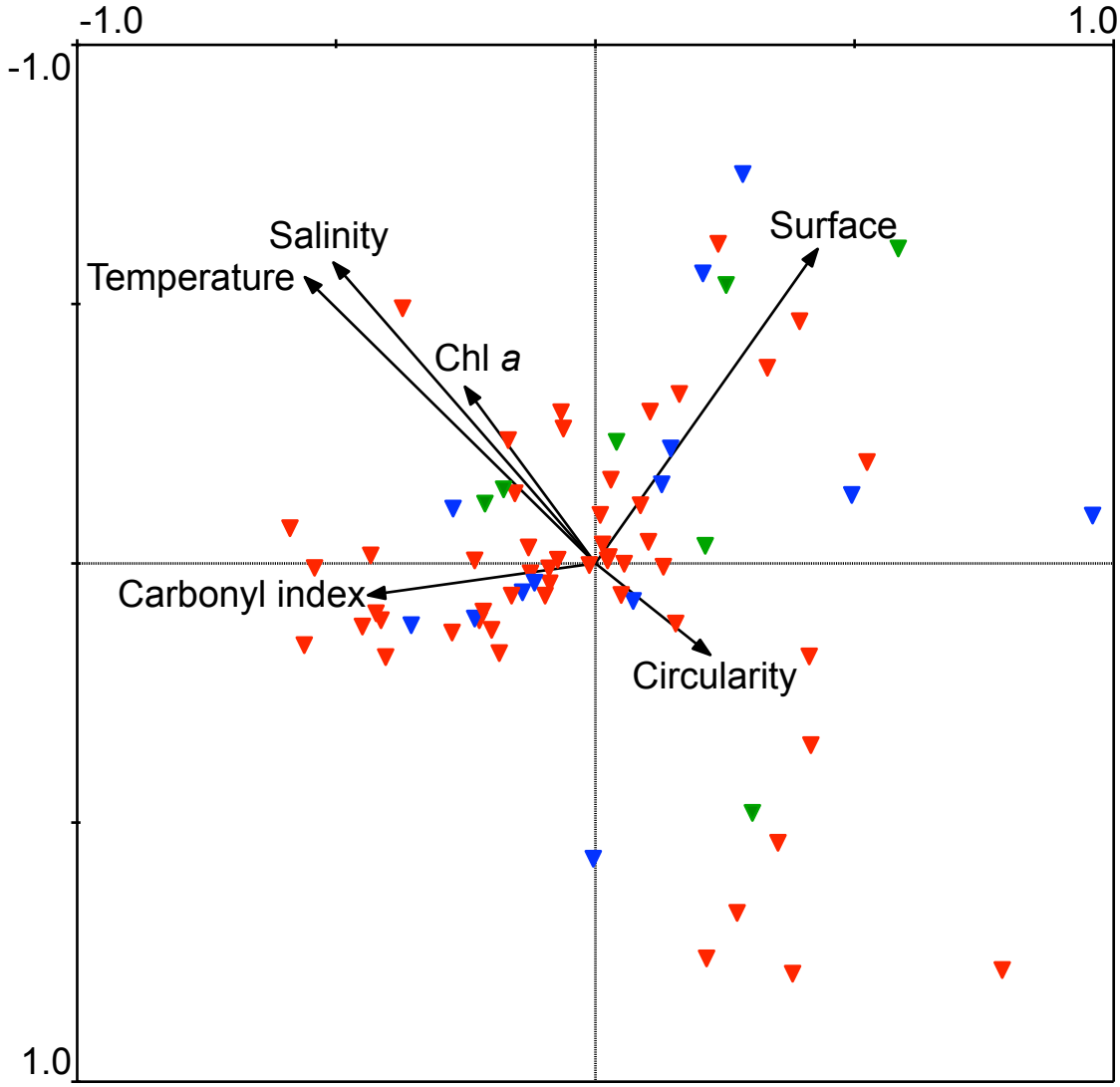

Supl. Figure S1: Canonical correspondence analysis of bacterial community structures living on plastics in relation to plastic characteristics (surface, shape and carbonyl index) and environmental variables (temperature, salinity, chlorophyll a, distance to the coast). Arrows point in the direction of increasing values of each variable and the length of the arrows indicates the degree of correlation with the represented axes. The first and second canonical axes explained 38 and 21% of the total variance, respectively. The remaining axes accounted for less than 13% of the total variance each and thus were not considered as significant enough.

Table S1: Contextual and physico-chemical data associated with the samples used in this study. PE: polyethylene, PP: polypropylene, PS: polystyrene, EVA: ethylene-vinyl acetate

Manta #	Study area	Latitude	Longitude	Distance to coast (km)	Composition	Shape	Color	Major size (mm)	Surface (mm^2)	Circularity	Carbonyl Index	Temperature	Salinity	Chl-a
M10P1	French Riviera (Monaco)	43.71	7.43	2.13	PE	pellet	white	4.92	15.77	0.67	1.61	ND	ND	ND
M10P2	French Riviera (Monaco)	43.71	7.43	2.13	PE	thick sheet	green	8.19	14.14	0.30	6.48	ND	ND	ND
M10P3	French Riviera (Monaco)	43.71	7.43	2.13	PE	sheet	white	11.67	56.43	0.19	9.84	ND	ND	ND
M15P3	Ligurian coast (Vintimiglia)	43.70	7.80	12.52	PE	sheet	white	13.37	88.43	0.16	10.66	ND	ND	ND
M15P4	Ligurian coast (Vintimiglia)	43.70	7.80	12.52	PP	sheet	transparent	17.31	164.10	0.46	8.06	ND	ND	ND
M19P1	French Riviera (Nice)	43.64	7.21	0.30	EVA	sheet	transparent	12.83	64.05	0.62	23.16	ND	ND	ND
M19P2	French Riviera (Nice)	43.64	7.21	0.30	Composite	sheet	white	21.04	234.02	0.52	43.09	ND	ND	ND
M20P1	French Riviera (Open sea)	43.46	7.54	28.82	PE	sheet	transparent	7.33	32.04	0.55	18.81	ND	ND	ND
M20P4	French Riviera (Open sea)	43.46	7.54	28.82	PE	sheet	transparent	5.02	16.05	0.75	23.86	ND	ND	ND
M20P6	French Riviera (Open sea)	43.46	7.54	28.82	PP	sheet	transparent	15.88	49.10	0.25	23.20	ND	ND	ND
M32P1	Gulf of Lions (Portoferraio)	42.86	10.18	5.15	PE	sheet	white	10.34	44.17	0.39	10.37	23.94	37.93	0.05
M32P2	Gulf of Lions (Portoferraio)	42.86	10.18	5.15	PE	pellet	white	6.28	22.25	0.60	13.49	23.94	37.93	0.05
M32P5	Gulf of Lions (Portoferraio)	42.86	10.18	5.15	PE	sheet	transparent	18.89	67.52	0.17	5.00	23.94	37.93	0.05
M32P6	Gulf of Lions (Portoferraio)	42.86	10.18	5.15	PE	sheet	transparent	6.46	16.51	0.38	8.08	23.94	37.93	0.05
M38P3	Gulf of Saint-Florent	42.82	9.29	2.85	PE	pellet	white	9.35	27.83	0.25	4.01	22.79	38.01	0.03
M42P1	Gulf of Saint-Florent (Open sea)	42.97	8.94	32.82	PE	sheet	transparent	3.41	8.34	0.56	17.39	23.21	38.09	0.04
M42P2	Gulf of Saint-Florent (Open sea)	42.97	8.94	32.82	PE	thick sheet	transparent	3.83	7.09	0.55	17.69	23.21	38.09	0.04
M42P3	Gulf of Saint-Florent (Open sea)	42.97	8.94	32.82	PE	sheet	transparent	7.21	12.63	0.31	9.94	23.21	38.09	0.04
M47P3	Tyrrhenian Sea (East Corsica)	42.26	9.66	8.59	PE	thick sheet	white	5.74	17.00	0.30	22.00	23.57	37.75	0.05
M47P5	Tyrrhenian Sea (East Corsica)	42.26	9.66	8.59	PE	sheet	white	6.07	16.57	0.30	14.90	23.57	37.75	0.05
M47P6	Tyrrhenian Sea (East Corsica)	42.26	9.66	8.59	PE	sheet	transparent	6.26	17.71	0.39	8.15	23.57	37.75	0.05
M51P2	Tyrrhenian Sea (East Corsica)	41.95	9.98	46.49	PP	sheet	transparent	5.59	17.63	0.62	8.85	24.06	37.87	0.03
M51P4	Tyrrhenian Sea (East Corsica)	41.95	9.98	46.49	PE	thick sheet	transparent	4.50	10.93	0.48	15.38	24.06	37.87	0.03
M56P1	Strait of Bonifacio (south Corsica)	41.37	9.17	0.65	Composite	sheet	white	9.95	50.25	0.42	15.82	22.27	38.04	0.04
M56P2	Strait of Bonifacio (south Corsica)	41.37	9.17	0.65	Composite	sheet	transparent	5.59	17.51	0.51	7.88	22.27	38.04	0.04
M60P1	Tyrrhenian Sea (East Sardinia)	41.04	10.66	94.45	PP	sheet	transparent	9.89	55.72	0.31	7.69	22.88	38.14	0.04
M60P4	Tyrrhenian Sea (East Sardinia)	41.04	10.66	94.45	PE	sheet	transparent	13.22	39.25	0.34	17.14	22.88	38.14	0.04
M60P5	Tyrrhenian Sea (North Sicily)	41.04	10.66	94.45	PE	sheet	transparent	8.21	17.78	0.24	1.92	22.88	38.14	0.04
M66P1	Tyrrhenian Sea (North Sicily)	39.00	12.42	68.01	PE	sheet	transparent	5.01	10.93	0.54	16.40	24.61	37.63	0.03
M66P2	Tyrrhenian Sea (North Sicily)	39.00	12.42	68.01	PE	pellet	transparent	4.39	13.68	0.65	24.30	24.61	37.63	0.03
M66P5	Tyrrhenian Sea (North Sicily)	39.00	12.42	68.01	PE	pellet	transparent	2.84	4.53	0.63	14.73	24.61	37.63	0.03
M165P1	Tyrrhenian Sea (Palermo)	38.27	13.82	32.52	PP	sheet	transparent	21.24	166.11	0.54	8.66	27.56	37.78	0.05
M165P3	Tyrrhenian Sea (Palermo)	38.27	13.82	32.52	PP	sheet	transparent	23.80	132.74	0.38	12.91	27.56	37.78	0.05
M165P5	Tyrrhenian Sea (Palermo)	38.27	13.82	32.52	PE	sheet	transparent	6.23	7.24	0.52	10.12	27.56	37.78	0.05
M173P1	Southeast of Algerian Basin	37.36	7.15	30.04	PE	sheet	blue	14.06	88.99	0.36	9.46	26.41	37.36	0.04
M173P2	Southeast of Algerian Basin	37.36	7.15	30.04	PE	sheet	transparent	17.19	83.78	0.32	7.56	26.41	37.36	0.04
M173P3	Southeast of Algerian Basin	37.36	7.15	30.04	PE	sheet	orange	6.00	17.44	0.36	93.19	26.41	37.36	0.04
M173P4	Southeast of Algerian Basin	37.36	7.15	30.04	PE	sheet	transparent	13.55	48.53	0.38	23.58	26.41	37.36	0.04
M178P2	Algerian Basin (Algiers)	37.73	3.80	91.86	PE	sheet	black	2.97	5.26	0.31	7.32	25.90	36.81	0.08
M178P3	Algerian Basin (Algiers)	37.73	3.80	91.86	PP	sheet	transparent	8.18	9.14	0.38	14.70	25.90	36.81	0.08
M178P4	Algerian Basin (Algiers)	37.73	3.80	91.86	PE	sheet	white	6.79	23.26	0.51	5.85	25.90	36.81	0.08
M189P1	Algerian Basin (Balearic Islands)	39.51	5.17	83.34	PE	thick sheet	white	7.87	24.94	0.29	12.46	26.37	37.46	0.02
M189P2	Algerian Basin (Balearic Islands)	39.51	5.17	83.34	PE	sheet	transparent	13.93	86.81	0.20	7.76	26.37	37.46	0.02
M189P3	Algerian Basin (Balearic Islands)	39.51	5.17	83.34	PE	sheet	transparent	8.24	17.90	0.36	17.48	26.37	37.46	0.02
M193P1	Algerian Basin (Balearic Islands)	40.47	5.27	100.01	PE	sheet	yellow	12.55	113.84	0.20	21.71	25.83	37.82	0.04
M193P2	Algerian Basin (Balearic Islands)	40.47	5.27	100.01	PE	pellet	light pink	10.57	14.95	0.30	14.10	25.83	37.82	0.04
M193P3	Algerian Basin (Balearic Islands)	40.47	5.27	100.01	PE	sheet	transparent	7.21	29.35	0.30	5.23	25.83	37.82	0.04
M193P4	Algerian Basin (Balearic Islands)	40.47	5.27	100.01	PE	sheet	blue	6.99	10.67	0.34	6.67	25.83	37.82	0.04
M202P1	Gulf of Lions (Marseille)	43.26	5.34	2.04	Composite	sheet	transparent	19.13	118.52	0.40	3.19	22.46	38.28	0.04
M202P2	Gulf of Lions (Marseille)	43.26	5.34	2.04	PS	sheet	transparent	7.22	36.46	0.46	22.00	22.46	38.28	0.04
M202P3	Gulf of Lions (Marseille)	43.26	5.34	2.04	PS	sheet	transparent	8.21	31.88	0.42	21.77	22.46	38.28	0.04
M234P1	Tyrrhenian Sea (Naples)	40.62	13.74	13.89	PP	sheet	white	7.00	17.03	0.45	12.82	23.87	37.90	0.04
M234P2	Tyrrhenian Sea (Naples)	40.62	13.74	13.89	PP	sheet	transparent	10.57	49.34	0.60	11.70	23.87	37.90	0.04
M238P5	Tyrrhenian Sea (Naples)	40.71	14.12	11.54	PP	sheet	transparent	9.39	38.24	0.48	11.80	23.78	37.95	0.04
M238P6	Tyrrhenian Sea (Naples)	40.71	14.12	11.54	PE	sheet	white	7.43	28.70	0.11	6.48	23.78	37.95	0.04
M238P7	Tyrrhenian Sea (Naples)	40.71	14.12	11.54	PE	sheet	transparent	6.03	20.87	0.39	10.98	23.78	37.95	0.04
M263P1	Gulf of Lions (Perpignan)	42.49	3.45	25.37	PE	sheet	white	12.49	70.84	0.34	11.22	22.26	38.24	0.03
M263P10	Gulf of Lions (Perpignan)	42.49	3.45	25.37	PE	thick sheet	white	3.02	5.05	0.40	8.91	22.26	38.24	0.03
M269P2	Balearic Sea (Barcelona)	41.23	2.13	6.87	PE	pellet	white	5.15	19.29	0.55	16.80	21.56	38.18	0.05
M269P3	Balearic Sea (Barcelona)	41.23	2.13	6.87	PE	sheet	green	10.57	66.04	0.30	7.54	21.56	38.18	0.05
M277P4	Balearic Sea (Gulf of Valencia)	39.00	0.77	55.73	PE	sheet	transparent	15.29	109.20	0.34	6.53	21.67	38.18	ND
M277P6	Balearic Sea (Gulf of Valencia)	39.00	0.77	55.73	PE	sheet	white	4.12	9.86	0.50	6.91	21.67	38.18	ND
M280P2	Balearic Sea (Costa Blanca)	38.27	-0.28	44.11	PP	sheet	green	7.31	17.82	0.37	14.07	23.07	38.07	ND
M280P5	Balearic Sea (Costa Blanca)	38.27	-0.28	44.11	PE	sheet	white	8.10	37.90	0.40	11.90	23.07	38.07	ND
M280P7	Balearic Sea (Costa Blanca)	38.27	-0.28	44.11	PE	sheet	white	4.12	4.78	0.40	19.61	23.07	38.07	ND
M283P4	Balearic Sea (Cartagena)	37.48	0.73	126.92	PP	sheet	transparent	9.10	49.41	0.24	18.97	22.10	37.92	ND
M283P5	Balearic Sea (Cartagena)	37.48	0.73	126.92	PE	pellet	transparent	4.05	10.71	0.44	22.25	22.10	37.92	ND
M283P6	Balearic Sea (Cartagena)	37.48	0.73	126.92	PE	sheet	transparent	8.65	25.85	0.23	25.30	22.10	37.92	ND
M285P1	Alboran Sea (Strait of Gibraltar)	36.12	-5.04	26.37	PE	sheet	white	15.05	127.58	0.05	13.92	18.46	36.43	ND
M285P4	Alboran Sea (Strait of Gibraltar)	36.12	-5.04	26.37	PE	sheet	transparent	9.59	57.38	0.42	4.49	18.46	36.43	ND
M285P5	Alboran Sea (Strait of Gibraltar)	36.12	-5.04	26.37	PP	sheet	transparent	9.77	46.43	0.45	4.97	18.46	36.43	ND
M285P6	Alboran Sea (Strait of Gibraltar)	36.12	-5.04	26.37	PE	thick sheet	white	7.70	22.67	0.25	12.80	18.46	36.43	ND